OCEAN APPLICATIONS TECHNICAL NOTE 14

The Positioning of the North Atlantic Current

by

D K Wright and C Gordon

Met Office
FitzRoy Road, Exeter, Devon. EX1 3PB

The Positioning of the North Atlantic Current

D.K. Wright and C. Gordon

Ocean Applications Branch. Meteorological Office,
Bracknell, Berkshire, RG12 2SZ, UK.

Summary

The warm water advected by the North Atlantic Current (NAC) is important for the climate of Western Europe. A general overview of the current both from observations and modelling studies is presented followed by experiments to investigate the positioning of the NAC using a global 1.25° resolution Cox ocean model. Sensitivity experiments involving the input of anomalous buoyancy forcing in the Labrador and Irminger Basins showed the North Atlantic Current position to be sensitive to the surface buoyancy forcing in these regions and thus to the details of the thermohaline circulation.

1 Introduction

The North Atlantic Current (hereafter NAC - see table 1 for a full list of abbreviations used) is the extension of the Gulf Stream from where this warm current separates from the North American coast. Associated with this current is a frontal region of high horizontal sea surface temperature (SST) gradient. It is thought that the SST patterns in the North Atlantic, particularly in the Ratcliffe-Murray area near Newfoundland (Ratcliffe and Murray 1970), are significantly correlated to surface pressure patterns over both the Atlantic and Europe. Palmer and Zhaobo (1985) showed that SST anomalies in the Ratcliffe-Murray area could effect the storm tracks in the North Atlantic and thus can be important for the climate over Europe. Deser and Blackmon (1993) found that the observed time series of (winter time) sea ice concentration in the Davis Strait/Labrador Sea region is connected to the (winter time) SST time series east of Newfoundland with a correlation of -0.76 (i.e. more sea ice leads to colder SST) with the sea ice leading by two years (that is, changes in the sea ice occur two years before those in SST). This suggests that changes in the state of the Labrador Sea region may affect the SST near the Ratcliffe-Murray area (and therefore, the climate over the North Atlantic) with a lag of around 2 years.

The general track of the NAC is thought (e.g. Schmitz and McCartney 1993) to separate from the North American coast at Cape Hatteras where it then heads north eastwards around the Grand Banks. It then bifurcates with one component becoming the Azores current which recirculates southwards as a broad drift. The other turns sharply north travelling just to the east of the Grand Banks before reseparating at the Flemish Cap. It then tracks generally eastwards as a much broader, filamentary current toward the eastern side of the Atlantic basin.

Previous work shows that the position of the NAC, and in particular its path as it flows close to the Grand Banks is not well modelled, even in eddy resolving models. Roberts *et al* (1996) use a version of the Cox ocean model (Cox 1984) with a resolution of 1° by 1° and a model domain in the North Atlantic of 20°S to 82°N and describe the position of the NAC in their model in detail. After 30 years of model integration the simulated NAC had become too zonal in nature to a position east of the mid-Atlantic ridge where it turned northwards. Roberts *et al* (1996) also describe the results from a parallel integration of AIM (Atlantic Isopycnal Model), an implementation of the Miami

Isopycnic-Coordinate Ocean Model (Bleck *et al* 1992). They show (their fig 2a) that AIM continues to capture the general position of the NAC to the end of its 30 year integration. Beyond the Grand Banks the AIM simulation of the NAC follows a general north easterly track past the Charlie Gibbs Fracture Zone at 33°W 52°N. It then continues north easterly until bifurcating just southeast of Iceland. Roberts *et al* (1996) attribute these differences to the way each model treats the dense overflow waters flowing south through the Denmark Strait.

The Community Modelling Effort (CME) model as developed by Bryan and Holland (1989) is based on the primitive equation model developed by Bryan (1969) and Cox (1984). Böning *et al* (1995) use this model at three resolutions ranging from $\frac{1}{6}^\circ$ by $\frac{1}{5}^\circ$ to 1° by 1.2° to study the effects of deep water formation in the Greenland-Iceland-Norway (GIN) Sea. For the high resolution case, the simulated mean near-surface flow travels north between the Grand Banks and Flemish Cap until approximately 50°N where it turns eastward. Observations show that the NAC flows around the Grand Banks to the East of the Flemish Cap, rather than between the two. The model flow then travels in a generally easterly direction until it abruptly turns north at 31° to 32°W. The current then bifurcates at about 55°N, the easterly flow broadens into a more general drift whilst the stronger, initially westward, flow heads towards the Denmark Straits. The lower, non eddy resolving, resolution configuration also has a generally northward flow towards the Denmark Straits. The general flow from the central North Atlantic towards the Denmark Strait is not seen in observations; instead the current generally flows eastward until close to the shelf break off Ireland. This may be due to the model treatment of the northern boundary, which is at 65°N, in this model.

Semtner and Chervin (1992) also used a primitive equation model based on that of Bryan (1969) having a horizontal grid spacing of 0.5° and 20 levels in the vertical. The model has a global domain but is cut off at 65°N. This configuration also has the NAC moving north through the Flemish Pass in a similar way to the simulation of Böning *et al* (1995). The overall NAC direction is generally straight, with no marked northward turn around the Grand Banks as seen in observations.

The long term aim of the research described in the pages which follow is to produce an ocean model which is capable of being used as part of an Atmosphere-Ocean General Circulation Model in order to carry out transient climate prediction experiments. A good

simulation of the SST in the North Atlantic is important if an ocean model is to be used for this purpose. This paper aims to investigate the reasons why the modelled and observed positions of the NAC differ and also to point to the factors determining the position of the NAC's course across the North Atlantic, concentrating on the process of diapycnal mixing over sills.

In Section 2 we give an overview of the observed flows in the North Atlantic. An outline of the problem of modelling flows over sills is given in section 3. Section 4 gives a brief description of the model used for the experiments performed which are described in section 5. Finally, section 6 draws some conclusions and discusses the issues raised by these experiments.

2 The Flow in the North Atlantic

The North Atlantic is the most highly observed ocean basin in the world. Schmitz and McCartney (1993) give a thorough description of current knowledge of the general circulation.

Figure 1, from Schmitz and McCartney (1993), shows three schematic diagrams of the circulation in the North Atlantic for water in different temperature bands. Figures in circles denote the along-path transport in Sv ($1Sv=10^6 m^3 s^{-1}$), whilst figures in squares denote sinking and dotted lines show water undergoing cooling. Figure 1a shows the circulation for temperatures $\geq 7°C$. This figure suggests that the Gulf Stream bifurcates with 12 Sv heading north as the NAC, 17 Sv recirculating in the Azores current and 1 Sv crossing the Atlantic to eventually enter the Mediterranean to be converted into Mediterranean outflow water. Figure 1b shows a schematic representation of the intermediate (4°C-7°C) water flow. Schmitz and McCartney (1993) point out that the flows at this level are the least well known and so are still open to some debate. The 12 Sv of water associated with the NAC can be seen turning northwards near to the Grand Banks, before traversing the North Atlantic in a general northeastwards direction. A total of 5 Sv overflows into the GIN sea where it sinks to form deep water. There is a recirculating gyre in the northern North Atlantic of subpolar mode water of 14 Sv. This gyre has a 'source' from the NAC and a 'sink' of 7 Sv sinking to a deeper level in the Labrador Sea.

Flows over the Denmark Straits and Iceland-Scotland Ridge are particularly important

for the thermohaline circulation. Intense cooling and some freshening means the dense outflows are much colder and significantly fresher than the warm inflows. These outflows are important in the renewal of North Atlantic Deep Water (NADW). Dickson and Brown (1994) used several long-term current meter arrays to measure flow of deep water ($\sigma_\theta >$ 27.8) off the east coast of Greenland. They used these results, along with earlier studies, to show that 2.9 Sv overspills the Denmark Strait. This flow rapidly increases to 5.2 Sv close to the ridge due to entrainment into the overflow water of the less dense water to the south of the ridge. It then increases to around 13.3 Sv (15 Sv in figure 1 from Schmitz and McCartney 1993) as the current rounds Cape Farewell. This further increase is due to inclusion of deep water (Labrador Sea Water and deep water flowing over the Iceland-Scotland ridge) and Antarctic Bottom Water recirculating in a loop between the Irminger and Labrador basins. Some of this water would also be entrained into the deep western boundary current (DWBC) and thus be lost southwards.

There is also a flow of deep water from overspills through the Faroe Bank Channel and the Iceland-Faroe ridge plus a component of Lower Deep Water due to Antarctic Bottom Water spreading north up the eastern half of the North Atlantic Basin. Dickson and Brown (1994) give a representative figure of 1.7 Sv for the Faroe Bank Channel through flow. Meincke (1983) gives an estimate of 1 Sv for the outflow along the Iceland-Faroes ridge. There is also 3.9 Sv of Lower Deep Water (McCartney 1992) of Antarctic Bottom Water origin which turns west at the northern end of the eastern North Atlantic basin. Despite all the deep flows, Saunders (1994) only observes 2.4 Sv of deep water flow through the Charlie Gibbs Fracture Zone.

These deeper flows are summarised in figure 1c, which shows the flows in the temperature range 1.8° - 4°C from Schmitz and McCartney (1993). They also suggest a flow of around 5 Sv throught the Charlie Gibbs Fracture Zone, much larger than the later paper of Saunders (1994), showing that ideas on the North Atlantic circulation are still being updated.

3 Modelling dense overflows

As demonstrated by Roberts *et al* (1996), the waters that overflow the Greenland-Iceland-Scotland ridge through the Denmark Strait are not well simulated in a level model such as

the Cox model. In reality the overflows flow down the bottom slope underneath the lighter water, thus maintaining their T/S characteristics. In a level model, however, the waters tend to be mixed together, giving a single mass of water with an intermediate density. There are two possible reasons for this. The first is due to convective mixing, if denser water overlies lighter water each box is mixed with the box below it until the water column is stable. The second means by which this mixing can happen is due to the isopycnal mixing scheme used in the model. The diffusion scheme used in the experiments described below is that of Redi (1982) (as implemented by Cox 1987). For numerical reasons, this scheme requires a maximum slope of the isopycnals to be set. If the actual slope exceeds this maximum then the isopycnal diffusion is held at this maximum level giving an implicit diapycnal mixing. In regions of large horizontal changes in density (such as the overflow regions) the isopycnals are very steep and so this can mean a large diapycnal component to the isopycnal diffusion. This is illustrated schematically in figure 2, reproduced from Roberts *et al* (1996) who discuss this problem and conclude that this was the dominant factor for the overflow waters becoming too warm and salty in their model. However, they also point out that including an improvement to the isopycnal scheme due to Gerdes *et al* (1991), which eliminates any diapycnal mixing due to the isopycnals sloping too steeply, gave no appreciable improvement in the overflow simulation. This suggests that if diapycnal mixing due to the isopycnal scheme is removed, the convective mixing scheme will take over as the dominant diapycnal mixing source.

Roberts *et al* (1996) suggest that these problems with the overflow waters cause the build up of anomalously light water in the northern North Atlantic seen in their model. The lightness of the resultant water mass preventing it from escaping south in the DWBC as this current rounds the Grand Banks. This large water mass then fills the sub polar gyre to the north of the NAC from a depth of around 200m to near the bottom. Roberts *et al* (1996) suggest this as a possible reason for the increased zonality of the NAC seen in their model with the build up of a large homogeneous layer of water in the central North Atlantic 'pushing' the NAC further southwards. This mechanism is investigated further in the next sections.

4 Model Description

The experiments described below were aimed at investigating the simulation of the NAC in the light of previous modelling experience (e.g. Roberts *et al* 1996). In particular how the NAC responds to possible changes to the simulation of dense overflow water across the Greenland Scotland ridge.

The model used for these experiments was that of Cox (1984) with the inclusion of a number of additional physical parametrizations. The model's domain was fully global with a horizontal grid resolution of 1.25° in both the zonal and meridional directions giving a total of 144 by 288 grid points. There were 20 levels in the vertical with a higher density of levels near the surface to resolve the mixed layer and thermocline (see table 2 for the exact depths of each level).

Vertical mixing near the ocean surface was represented by an embedded Kraus-Turner mixed layer model (Kraus and Turner 1967) and, in addition, a Richardson number dependent vertical diffusion (Pacanowski and Philander 1981). The horizontal diffusion was parametrized as a simple down gradient flux in the momentum and the tracer equations. The tracer diffusion employed the isopycnal mixing scheme of Redi (1982). A simple representation of sea-ice effect on surface exchange was used which shuts off surface fluxes if a surface grid box reaches the minimum allowed temperature of -1.8°C.

The topography was taken from the ETOPO5 (1988) $\frac{1}{12}^{\circ}$ resolution dataset interpolated onto the model grid, this was then put through a simple 'del squared' smoother twice to produce the topography used in the model. Roberts and Wood (1997) showed that Bryan-Cox type models are highly sensitive to the depth of the various channels along the Greenland-Scotland ridge. Many of these channels are subgridscale and so three routes (one grid point wide on the velocity grid) through the ridge were excavated: The Denmark Strait and Iceland-Faroes ridge were reduced to 797.9m (bottom of model level 12), while the Faroe-Scotland ridge was set to 534.7m (bottom of model level 11). This gave an outflow through the Denmark Strait of approximately 7 Sv averaged over the first year, compared to that observed of around 5-6 Sv (Dickson and Brown 1994).

With the eventual use of this model as part of a coupled Atmosphere-Ocean General Circulation Model in mind, a land-sea mask identical to that for the Hadley Centre atmospheric climate model was imposed. This has a resolution of 2.5° x 3.75°. Figure 3 shows the resulting model bathymetry and land-sea mask for the North Atlantic.

The control run of the model was forced with Hellerman and Rosenstein (1983) wind-stress, Esbensen and Kushnir (1981) heat fluxes and Jaeger (1976) precipitation minus Esbensen and Kushnir (1981) evaporation. These forcing fields included a seasonal cycle with 12 monthly values and a linear time interpolation used between them. For the surface heat flux a Newtonian relaxation similar to that of Haney (1971) was used:

$$Q_{appl} = Q_{obs} + \lambda(T_{clim} - T_{mod})$$

Where Q_{appl} is the net heat flux applied to the model, Q_{obs} is the observed heat flux, λ is the relaxation coefficient (set to $35\mathrm{Wm}^{-2}\mathrm{K}^{-1}$giving a relaxation timescale of 68 days for a 50m layer), T_{clim} is the climatological SST and T_{mod} the model SST. This equation is derived from a truncated Taylor expansion of the individual terms making up the applied heat flux (solar, longwave, sensible and latent heat) about a reference temperature (T_{clim}). Haney (1971) calculated a physical value of λ of around $40\mathrm{Wm}^{-2}\mathrm{K}^{-1}$. An exactly analogous form for the restoring term is used for the fresh water forcing field using climatological and model sea surface salinity (SSS), with a relaxation coefficient chosen to give the same restoring timescale as for temperature. The climatological SST used in the model was taken from the Global Ice and Sea Surface Temperature dataset (GISST, Parker *et al* 1994) and the climatological sea surface salinity from Levitus (1982).

The model was initialised from rest with potential temperature and salinity for September from Levitus (1982). It was integrated for ten years and most of the charts depict annual means for the final tenth year.

5 Experiment description and results

Figure 4a shows the annual mean potential temperature from the Levitus (1982) climatology at model level 5 (47 m). The Levitus (1982) data clearly captures the general features associated with the NAC, with the tight temperature gradients off the east coast of the United States then curving northward past the Grand Banks until becoming more broad and zonal as the NAC moves eastwards across the central North Atlantic. Being a climate mean the temperature gradients are broader than would be expected from an instantaneous observed pattern of North Atlantic SST with the effects of the meanders and eddies associated with this current being smoothed out. The effect of strong surface cooling is evident in the GIN Sea which is associated with the large production of deep

water here. The extremely cold temperatures off Greenland are associated with the East Greenland Current.

The salinity at model level 5 (47m) from Levitus (1982) is shown in figure 4b. This also shows the strong salinity front associated with the NAC on the western side of the basin. There is also the extremely fresh water off the Labrador coast associated with melt water and Hudson Bay outflow.

The temperature structure at model level 5 (47m) from the control run of the 1.25° ocean model (figure 5a) has some differences from Levitus (1982). The model captures the tight temperature gradients associated with the NAC but the temperature structure associated with the NAC is far too zonal compared with Levitus giving differences of over 5°C in the central North Atlantic. Figure 5b shows the salinity at the same level from the model. This shows a related salinity gradient which is too zonal, leading to a large difference in salinity between the model and climatology. This large systematic error is seen in many other level models, showing it to be a robust feature in models of this type.

Figure 6a shows the temperature pattern for Levitus (1982) at model level 12 (666 m). This shows the Labrador Sea to generally have a temperature of near 4°C and that the tight gradients associated with the NAC are still visible at this depth. The Levitus (1982) salinity pattern at this depth (figure 6b) also shows a tight gradient across the path of the NAC and the Labrador and Irminger basins have a salinity of around 34.9 to 35.0 psu.

This contrasts with the temperature pattern of the control run at this depth (figure 7a), which has this 4° - 5°C water filling a large expanse of the central North Atlantic. The temperature gradients associated with the NAC are also still apparent at this depth and, like the near surface pattern, are also still far too zonal. The salinity pattern (figure 7b) also shows a similar feature with 34.9 - 35.0 psu salinity water pushing too far eastwards when compared with Levitus (1982) (figure 6b).

Roberts *et al* (1996) also discussed this feature in their model and suggested the build up of a homogeneous water mass in the northern North Atlantic as a possible cause. They also suggested mixing of overflow water from the GIN Sea into the North Atlantic as the reason for the build up of this water (see section 2). One possible way to stop diapycnal mixing from this source would be to stop water flowing through the ridges between the GIN Sea and the North Atlantic. Experiments in which the Denmark Straits is blocked

off, however, showed no real improvement in this aspect of the simulation. This was thought to be due to the deep water being then forced to be formed south of Iceland, implying incorrect T/S characteristics, leading again to a build up of water at mid-depth.

Passive tracer experiments (not shown) show that a large amount of the 4° - 5°C water that builds up in the central North Atlantic in the model is formed in both the Labrador and Irminger Basins. However, it is possible that this build up of water is merely a 'symptom' of the spurious zonal nature of the NAC or, alternatively, that the position of the NAC is pushed south by the build up of this water. If this water was forced to sink to a greater depth so that it could not influence the NAC then this would show whether this was the causal mechanism for its southwards movement. In order to test this hypothesis two experiments were devised.

In the first, an anomalous buoyancy forcing was included in the Labrador basin (experiment I) and in the second, in the Irminger Basin (experiment II). In each of these regions (see figure 3) the reference SST and SSS were modified so as to enhance sinking away from the surface. The reference SST was altered to 3°C and the reference SSS to 35.4 psu (giving a $\sigma_\theta = 28.2$). This compares with annual mean SST and SSS in these regions of approximately 3°C and 33.5 psu ($\sigma_\theta = 26.7$) in the Labrador Basin and 6°C and 34.9 psu ($\sigma_\theta = 27.5$) in the Irminger basin. The relaxation coefficient, λ, was set to 200 $Wm^{-2}K^{-1}$in these regions, corresponding to a relaxation timescale of 12 days for a 50m layer. This ensured that the forcing was strong enough to produce deep convection in the each of the regions in the two experiments. By forcing the water in each of these regions to sink below the level it attained in the control experiment the intention was that the sub polar gyre would nolonger be filled with a homogeneous water mass. The effect of this water on the NAC could then be assessed.

Figure 8a shows the temperature at model level 5 for the Labrador Sea sensitivity experiment (experiment I). This shows a marked difference in the positioning of the isotherms when compared to the control experiment (figure 5a). The strong temperature gradient associated with the NAC is now broader and separates slightly further south. It also includes a marked swing to the north in the Grand Banks region. This means the temperature errors in the central North Atlantic when compared to Levitus (1982) are significantly reduced (of order 2.5°C at this level). The northward turn in the tight density gradient associated with the NAC can also be seen in the plot of salinity at this

level (figure 8b).

The temperature difference between experiment I and the control run at model level 5 (figure 9a) shows the inclusion of an anomalous buoyancy flux in the Labrador Sea has the effect of cooling the entire region off the coast of America and Canada between Florida and Newfoundland, whilst warming a large region in the central North Atlantic. It shows that the entire western boundary current structure has been modified and there is a northward shift in the path of the NAC as it passes the Grand Banks. Salinity differences at this level (figure 9b) show the enhanced salinity being advected into the general path of the NAC and a general freshening off the coast of America.

At model level 12 there are also marked differences. Figure 10a shows the Labrador Sea experiment temperatures at this level. The large expanse of 4° - 5°C water has been reduced and the temperature gradients associated with the NAC still maintain the more northerly track at this level when compared with the control experiment (figure 7a). This is also clearly evident in the salinity at this depth (figure 10b). The front associated with the NAC now has a pronounced northward turn around the Grand Banks, unlike the control run (figure 7b), and is more similar to the front in Levitus (1982) (figure 6b).

Figures 11a and 11b show plots of temperature, salinity and density profiles versus the volume transport across a north/south section to the south of Newfoundland (see figure 3 for the exact position) for both the control and experiment I respectively. If it is assumed that this section captures all the DWBC flowing past this point, then this will show up as the westward flowing, cold, fresh and dense water in these plots. It can be seen that the strength of the DWBC has increased from around 4.7 Sv for the control run to 12.3 Sv in experiment I. This is now approaching the figure given by Schmitz and McCartney (1993) of 16 Sv of NADW rounding the Grand Banks in the DWBC. The change in T/S characteristics shows that the water flowing in the DWBC is slightly colder and more saline, giving a slightly more dense flow.

The inclusion of a large buoyancy forcing in the Labrador Sea, forcing deep convection in the region, might be expected to lead to a strong alteration to the thermohaline overturning in the north Atlantic. The formation and movement of water masses is also closely linked to the thermohaline circulation. We have already shown that an alteration to this circulation can effect the positioning of the NAC. However, has the thermohaline circulation now been altered so as to give an unrealistic overturning circulation?

One general way of looking at the thermohaline circulation is by comparing the meridional stream function. This is shown in figures 12a, the control run and 12b, the Labrador Sea anomaly experiment (experiment I). These figures show a strengthening of the main thermohaline cell in the North Atlantic from 16 to 24 Sv in experiment I. Roemmich and Wunsch (1985) estimate the southward NADW transport at 24°N to be 17 Sv, compared with 10-12 Sv for the control integration and 16-18 Sv for experiment I. Both experiments have cross equatorial transports which compare favourably with the estimate of Schmitz and Richardson (1991) of 13 Sv. Gerdes and Köberle (1995) found similar results to this in their experiment of increasing the buoyancy forcing applied in a region in the Denmark Strait. However, their meridional overturning increased by a much larger amount and there was a general deeping in the thermohaline cell. In their experiments they used an anomalous restoring temperature and salinity of 0.0°C and 34.95 psu respectively, giving $\sigma_\theta = 28.13$ (compared with 3.0°C and 35.4 psu, $\sigma_\theta = 28.2$ in the experiments described here). This suggests that the anomalous forcing applied need not have been so severe.

As has already been stated, the deeper flows are also affected by the inclusion of extra buoyancy forcing. This is apparent in figure 13, which shows the flows for model level 15 (2116 m). Both the control and experiment I show a similar lower circulation pattern. That is a boundary current flowing round Greenland and down the coast of Labrador before turning eastward and travelling across the width of the western Atlantic basin. The flow then heads southwestwards, passing south of the Grand Banks before travelling as a DWBC down the eastern seaboard of the United States. The velocity of the DWBC is considerably larger in the Labrador Sea anomaly experiment, however, showing that a considerable amount of deep water has now been forced to sink to a lower level and is flowing south in the DWBC. An east-west transport cross section at approximately 50°N across the Atlantic basin similar to figure 11 (not shown) confirms that the DWBC has indeed increased in strength here. This pattern of the deep flow is also seen in the 2.5° x 3.75° and 1° configurations of the Hadley Centre model. Figure 14 shows the difference in temperature between the control and Experiment I at this level. The anomaly experiment is both colder and saltier in the region of the DWBC showing that water which has been in contact with the buoyancy anomaly is now flowing southwards in the current. Another possibility is that the deep flows may enter the DWBC by flowing over the Grand Banks. This would require further investigation.

All the previous results were for an experiment where an anomalous buoyancy forcing was included in the Labrador Basin. The second experiment, in which the anomaly was included in the Irminger Sea gave broadly similar results to that of the Labrador Basin experiment. At the surface level the NAC was seen to now turn northward around the Grand Banks and the deeper levels showed a marked reduction in the amount of 4° - 5°C water present. The deep western boundary current was also much stronger, even than in the Labrador Sea experiment case, with 25 Sv flowing westward through the cross section shown in figure 3 compared to 12 Sv in the Labrador Sea experiment. The meridional stream function also showed a similar increase in overturning, with the maximum in the overturning cell now around 32 Sv. The cell also penetrates much deeper, to around 4000m. These much larger increases could be due either to the larger area over which the anomalous buoyancy forcing was included, meaning a much larger forcing was applied, or that the thermohaline circulation is much more sensitive to changes in density structure in the Irminger Sea compared to the Labrador Sea.

6 Summary

SST patterns in the North Atlantic (and especially the Ratcliffe-Murray area) are potentially important for climate over Europe. The zonality of the NAC is seen in many level models. In the model described here, there is a build up of 4° - 5°C water to the north of the NAC between 75 - 750m depths. This build up of water may, in part, be due to the poor representation of the overflow of dense water across the Denmark Strait. An inclusion of a scheme to help better represent the flow of dense waters down slopes, as opposed to simply mixing the waters, may help improve the simulation of NADW and Labrador Sea Water in the North Atlantic. Roberts *et al* (1996) included an improvement to the isopycnal diffusion scheme to avoid diapycnic mixing but this did not improve the simulation, possibly due to vertical convection mixing the water. A further source of diapycnic mixing is from the background horizontal diffusion required by the isopycnal diffusion scheme for numerical reasons. The parametrization due to Gent and McWilliams (1990) is an adiabatic mixing scheme and so may have a beneficial effect on the model's ability to maintain water masses over long timescale.

The inclusion of a surface buoyancy forcing anomaly in the Labrador Sea has the

effect of reducing the SST differences between the model and Levitus (1982) generally over the North Atlantic basin and the modelled NAC now takes a more northerly path. At lower depths the build up of 4° - 5°C water has been markedly reduced and the volume transport in the DWBC has increased 3 fold. It is evident from these experiments that the thermohaline circulation including the formation of deep water masses is important for the positioning and general course of the NAC and hence for the SST pattern in the North Atlantic.

References

Bleck, R., Rooth, C., Hu, D., and Smith, L. T., 1992: Salinity-driven thermocline transients in a wind- and thermohaline-forced isopycnic coordinate model of the North Atlantic. *J. Phys. Oceanogr.*, **22**, 1486–1505.

Böning, C. W., Bryan, F. O., Holland, W. R., and Doscher, R., 1995: Thermohaline circulation and poleward heat transport in a high-resolution model of the North Atlantic. Salinity-driven thermocline transients in a wind- and thermohaline-forced isopycnic coordinate model of the North Atlantic. *J. Phys. Oceanogr.* submitted.

Bryan, F. O. and Holland, W. R., 1989: A high resolution simulation of the wind- and thermohaline-driven circulation in the North Atlantic ocean. In: Parameterization of small-scale processes. Modelling of land surface processes and their influence on European climate. In *Proceeedings 'aha huliko'a, Hawaiian Winter Workshop*, 99–115.

Bryan, K., 1969: A numerical method for the study of the circulation of the world ocean. *J. Comput. Phys.*, **4**, 347–376.

Cox, M. D., 1984: A primitive equation, three dimensional model of the ocean. Ocean Group Technical Report 1, GFDL, Princeton.

Cox, M. D., 1987: Isopycnal diffusion in a z-coordinate model. *Ocean Modelling*, **74**, 1–5 (unpublished manuscript).

Deser, C. and Blackmon, M. L., 1993: Surface climate variations over the North Atlantic ocean during winter: 1900-1989. *Journal of Climate*, **6**, 1743–1753.

Dickson, R. R. and Brown, J., 1994: The production of North Atlantic deep water: sources, rates and pathways. *J. Geophys. Res.*, **99**, 12, 319–12, 341.

Esbensen, S. K. and Kushnir, Y., 1981: Heat budget of the global ocean: estimates from surface marine observations. Technical Report 29, Climate Research Institute, Oregon State University, Corvallis, Oregon, USA.

ETOPO5, 1988: Global 5'x5' depth and elevation. Technical report, National Geophysical Data Center, NOAA, U.S. Dept. of Commerce, Code E/GC3, Boulder, CO 80303, USA.

Gent, P. R. and McWilliams, J. C., 1990: Isopycnal mixing in ocean circulation models. *J. Phys. Oceanogr.*, **20**, 150–155.

Gerdes, R. and Köberle, C., 1995: On the influence of DSOW in a numerical model of the North Atlantic general circulation. *J. Phys. Oceanogr.*, **25**, 2624–2642.

Gerdes, R., Köberle, C., and Willebrand, J., 1991: The influence of numerical advection schemes on the results of ocean general circulation models. *Climate Dynamics*, **5**, 211–226.

Haney, R. L., 1971: Surface thermal boundary conditions for ocean circulation models. *J. Phys. Oceanogr.*, **1**, 241–248.

Hellerman, S. and Rosenstein, M., 1983: Normal monthly wind stress over the world ocean with error estimates. *Journal of Physical Oceanography*, **13**, 1093–1104.

Jaeger, L., 1976: Monatskarten des niederschlags fur die ganze erde. Technical Report 18, Number 139, Berichte des Deutshen Wetter Dienster, Offenbach, Germany.

Kraus, E. B. and Turner, J. S., 1967: A one dimensional model of the seasonal thermocline. Part II. *Tellus*, **19**, 98–105.

Levitus, S., 1982: Climatological atlas of the world ocean. Professional Paper 13, National Oceanic and Atmospheric Administration, Rockville, Maryland.

McCartney, M. S., 1992: Recirculating components to the deep boundary current of the northern North Atlantic. *Prog. Oceanogr.*, **29**, 283–383.

Meincke, J., 1983: The modern current regime across the Greenland-Scotland ridge. In Bott, A., B. Sakov, C. Talwani, and D.Thiode, editors, *Structure and development of the Greenland-Scotland ridge*, 637–650. Plenum, New York.

Pacanowski, R. C. and Philander, S. G., 1981: Parametrization of vertical mixing in numerical models of tropical oceans. *J. Phys. Oceanogr.*, **11**, 1443–1451.

Palmer, T. N. and Zhaobo, S., 1985: A modelling and observational study of the relationship between sea surface temperature in the north-west Atlantic and the atmospheric general circulation. *Quart. J. R. Met. Soc.*, **111**, 947–975.

Parker, D. E., Jones, P. D., Folland, C. K., and Bevan, A., 1994: Interdecadal changes of surface temperature since the late nineteenth century. *J. Geophys. Res*, **99**, 14373–14399.

Ratcliffe, R. A. S. and Murray, R., 1970: New lag associations between North Atlantic sea temperatures and European pressure, applied to long-range weather forecasting. *Quart. J. R. Met. Soc.*, **96**, 226–246.

Redi, M. H., 1982: Oceanic isopycnal mixing by coordinate rotation. *J. Phys. Oceanogr.*, **12**, 1154–1158.

Roberts, M. J. and Wood, R. A., 1997: Topography sensitivity studies with a Bryan-Cox type ocean model. *J. Phys. Oceanogr.*, **27**, 823–836.

Roberts, M. J., Marsh, R., New, A. L., and Wood, R. A., 1996: An intercomparison of a Bryan-Cox type ocean model and an isopycnic ocean model. Part I: The subpolar gyre and high-latitude processes. *J. Phys. Oceanogr.*, **26**, 1495–1527.

Roemmich, D. and Wunsch, C., 1985: Two transatlantic sections: meridional circulation and heat flux in the subtropical North Atlantic Ocean. *Deep-Sea Res.*, **32**, 619–664.

Saunders, P. M., 1994: The flux of overflow water through the Charlie-Gibbs Fracture Zone. *J. Geophys. Res.*, **99**, 12, 343–12, 355.

Schmitz, W. J. and McCartney, M. S., 1993: On the North Atlantic circulation. *Rev. Geophys.*, **31**, 29–49.

Schmitz, W. J. and Richardson, P. L., 1991: On the sources of the Florida Current. *Deep Sea Res.*, **38 suppl. 1**, s389–s409.

Semtner, A. J. and Chervin, R. M., 1992: Ocean general circulation from a global eddy-resolving model. *J. Geophys. Res.*, **97**, 5493–5550.

AIM	Atlantic Isopycnal Model
CME	Community Modelling Effort
DWBC	Deep Western Boundary Current
GIN	Greenland Iceland Norway
NAC	North Atlantic Current
NADW	North Atlantic Deep Water
SSS	Sea Surface Salinity
SST	Sea Surface Temperature

Table 1: List of abbreviations used

Model Level Number	Depth of level mid-point	Depth of level bottom	level thickness
1	5.0	10.0	10.0
2	15.0	20.0	10.0
3	25.0	30.0	10.0
4	35.0	40.2	10.2
5	47.8	55.5	15.3
6	67.0	78.5	23.0
7	95.7	113.0	34.5
8	138.9	164.8	51.8
9	203.7	242.6	77.8
10	301.0	359.4	116.8
11	447.0	534.7	175.3
12	666.3	797.9	263.2
13	995.5	1193.2	395.3
14	1500.8	1808.5	615.3
15	2116.1	2423.8	615.3
16	2731.3	3039.1	615.3
17	3346.6	3654.4	615.3
18	3961.9	4269.7	615.3
19	4577.1	4885.0	615.3
20	5192.4	5500.3	615.3

Table 2: Model Levels (metres)

Schematic diagram of the North Atlantic circulation
taken from Schmitz and McCartney (1993)

Figure 1a.

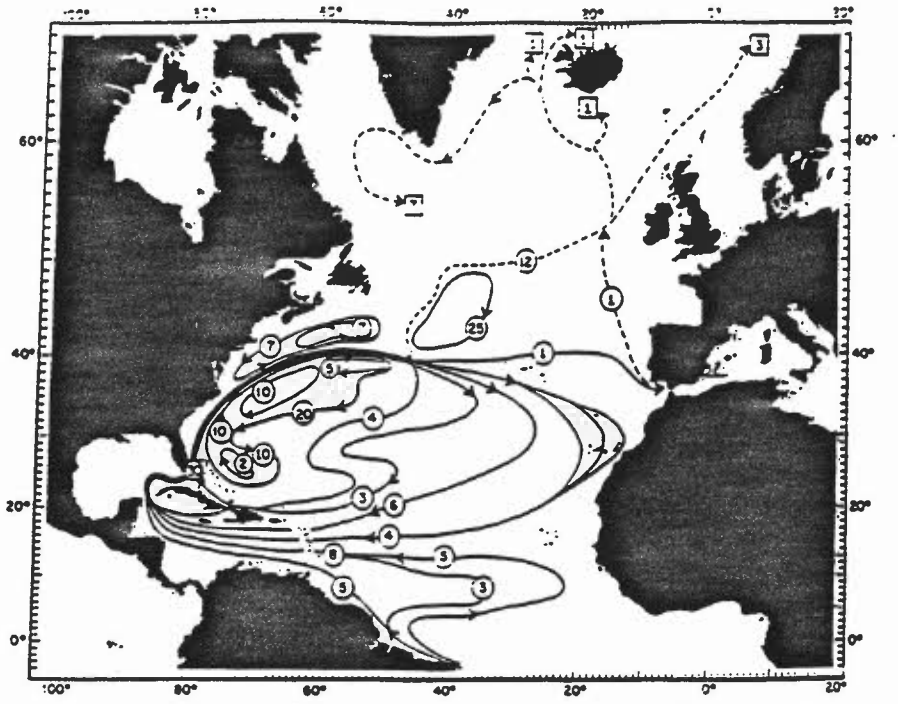

≥ 7°C

Figure 1b.

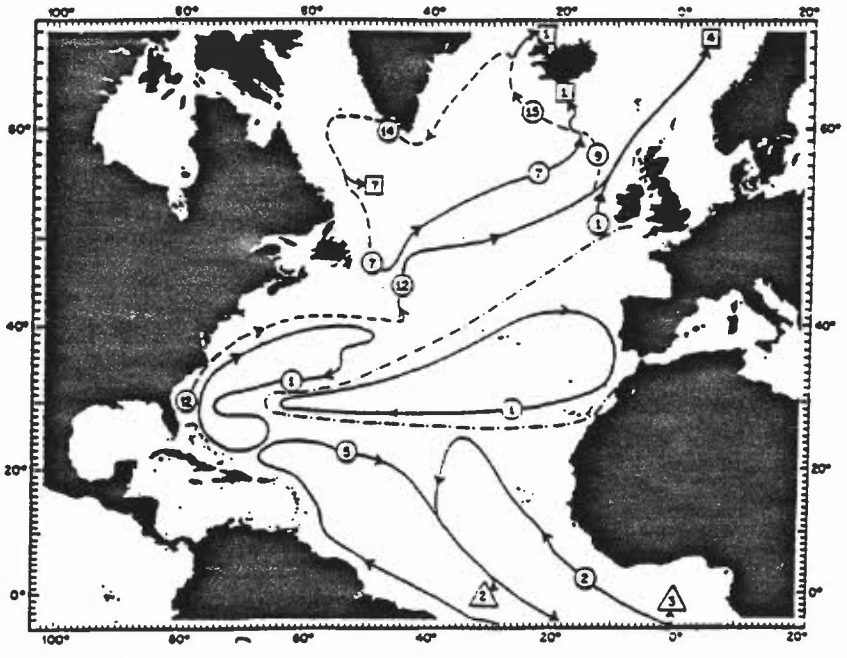

4° - 7°C

Figure 1c.

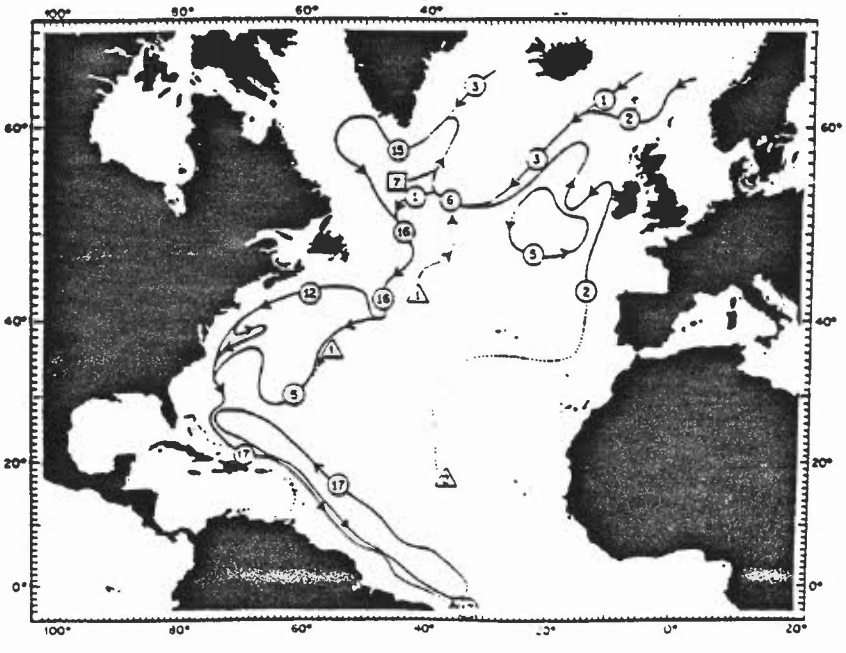

1.8° - 4°C

Δ = Upwelling.
O = Along path flow.
❑ = Sinking.

Schematic picture of a cross-section across a ridge with dense water on one side overflowing into a region of lighter water showing how the waters might mix due to factors involving the isopycan diffusion scheme.

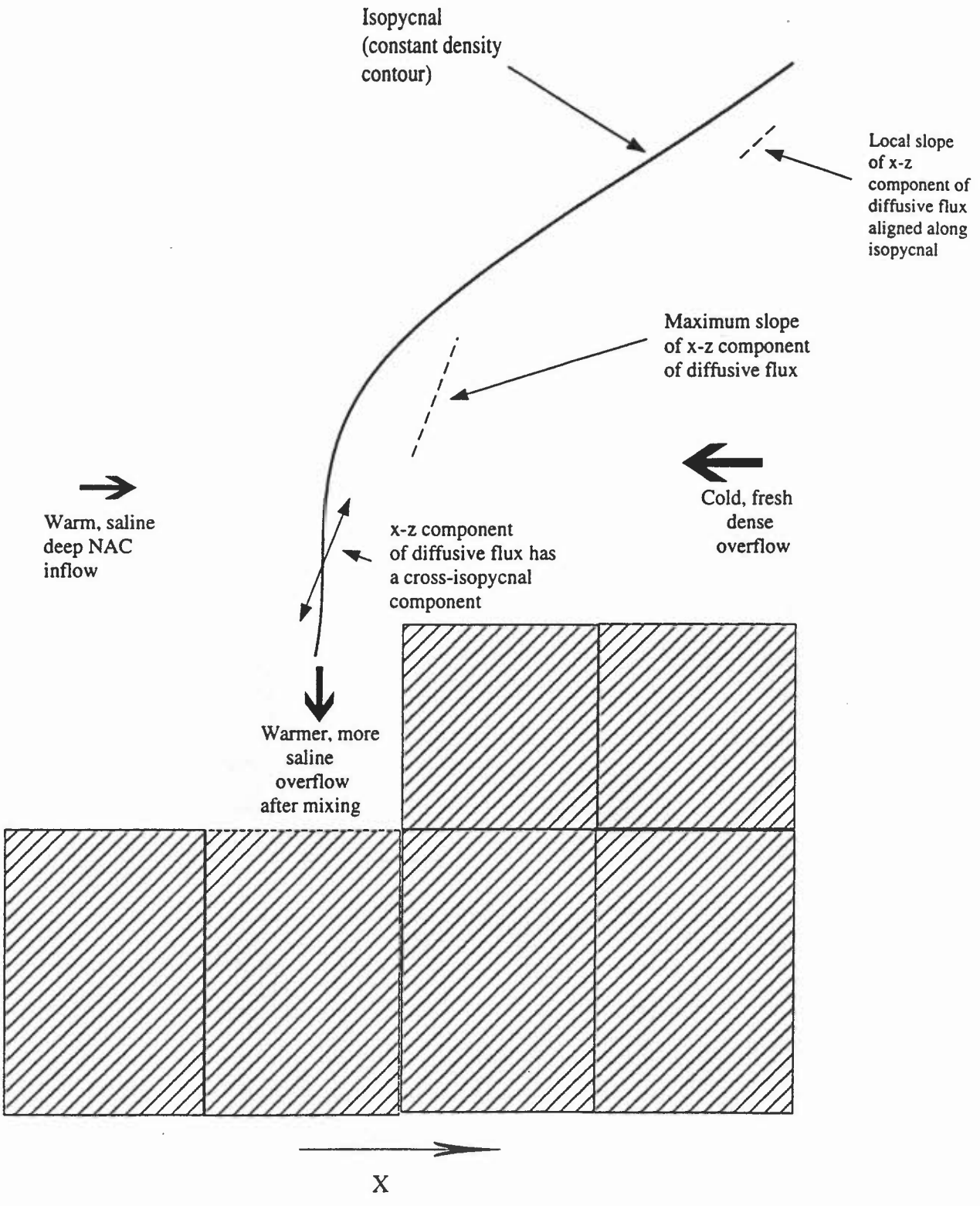

Figure 2

Model bathymetry (metres) of the North Atlantic.
Showing areas defined as Labrador and Irminger Basins
and cross section used.

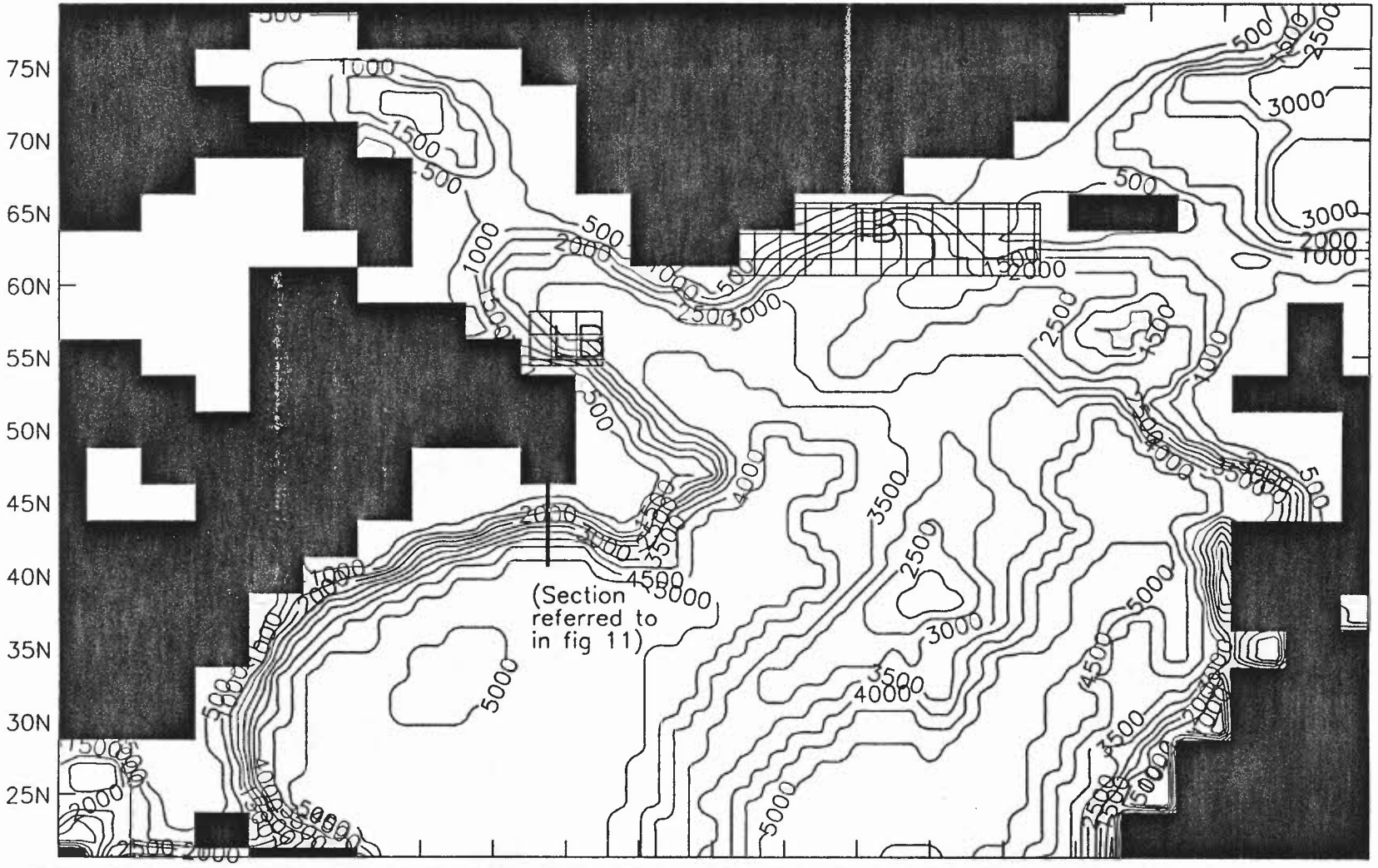

Figure 3.

Levitus (1982) annual mean potential temperature (°C).
Model level 5 (47m).

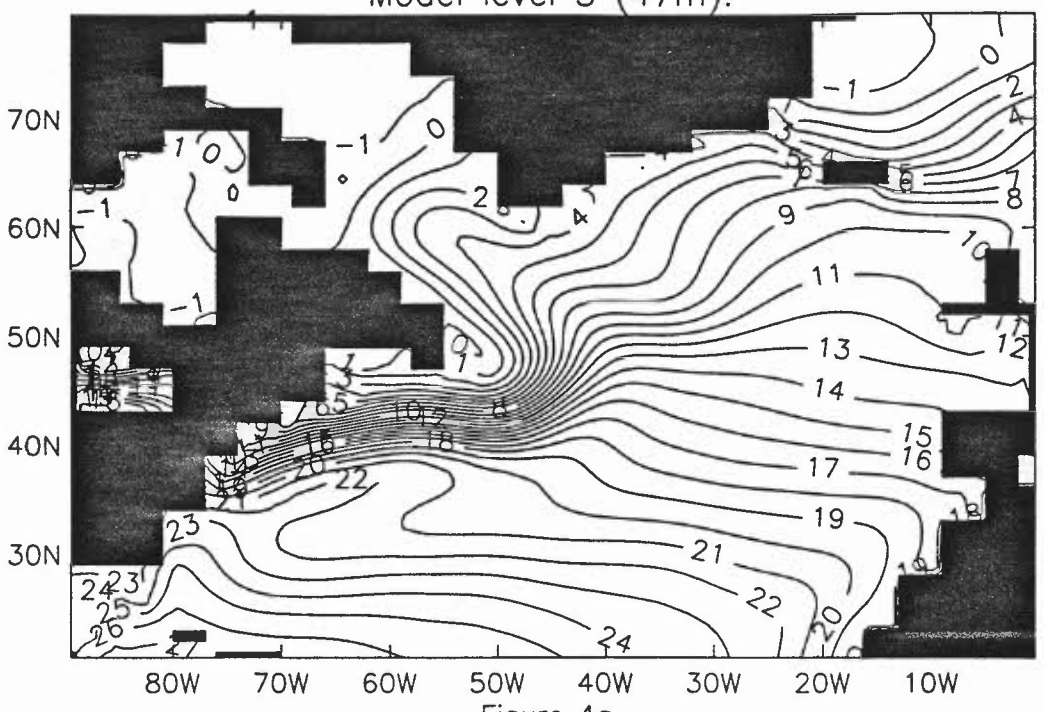

Figure 4a.

Levitus (1982) annual mean Salinity (psu).
Model level 5 (47m).

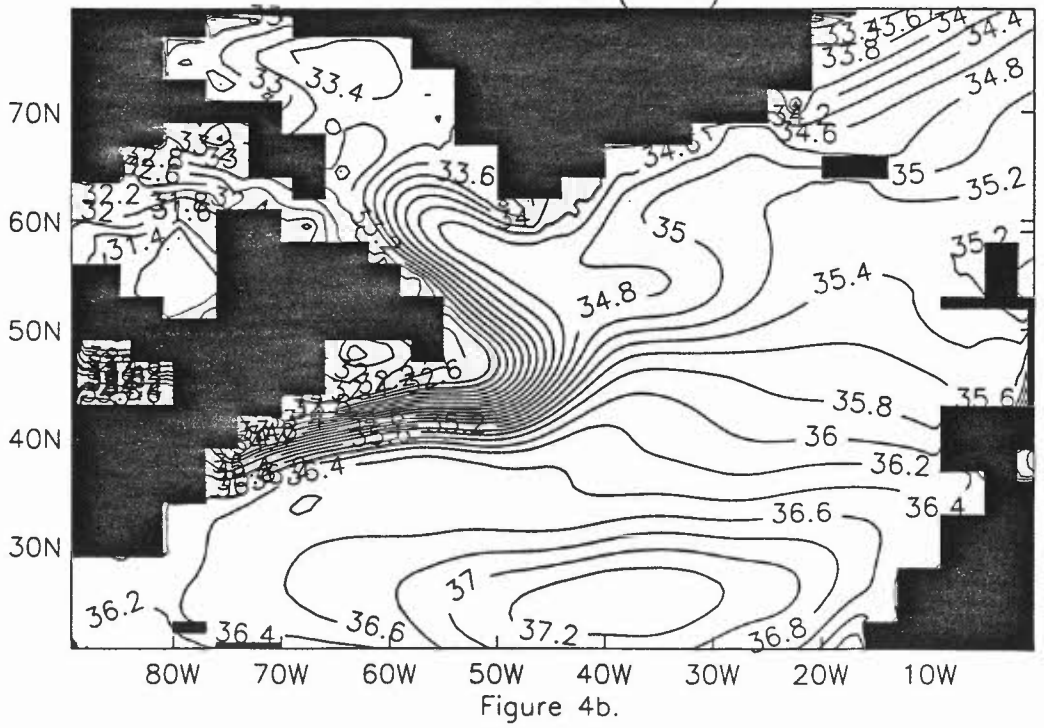

Figure 4b.

Control run annual mean potential temperature (°C).
Model level 5 (47m).

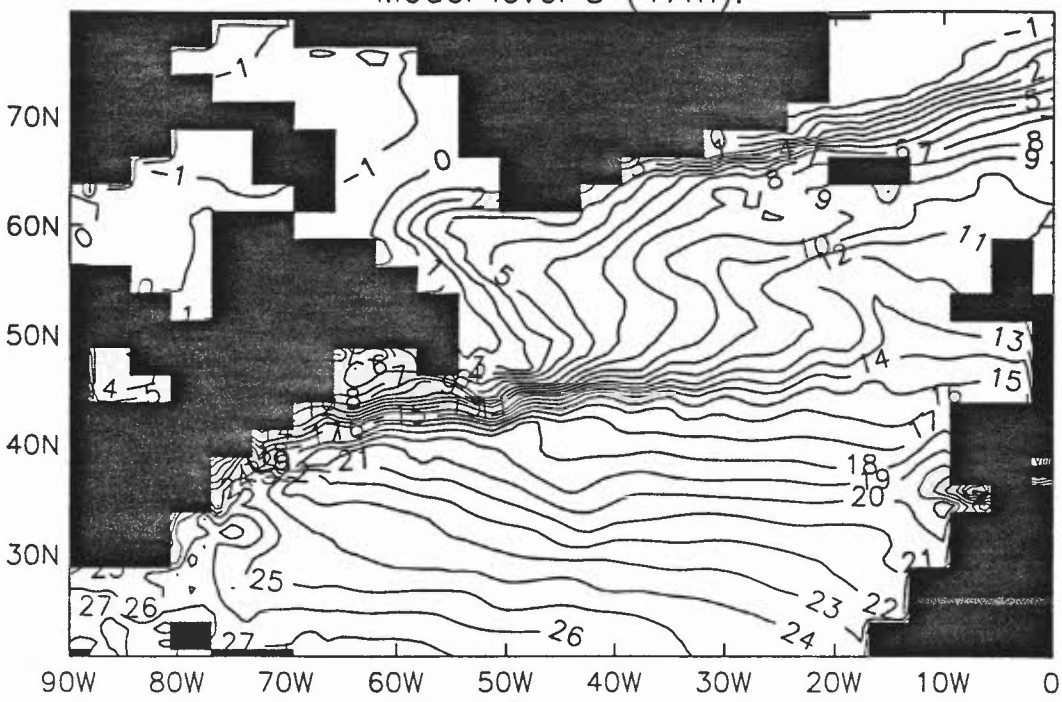

Figure 5a

Control run annual mean salinity (psu).
Model level 5 (47m).

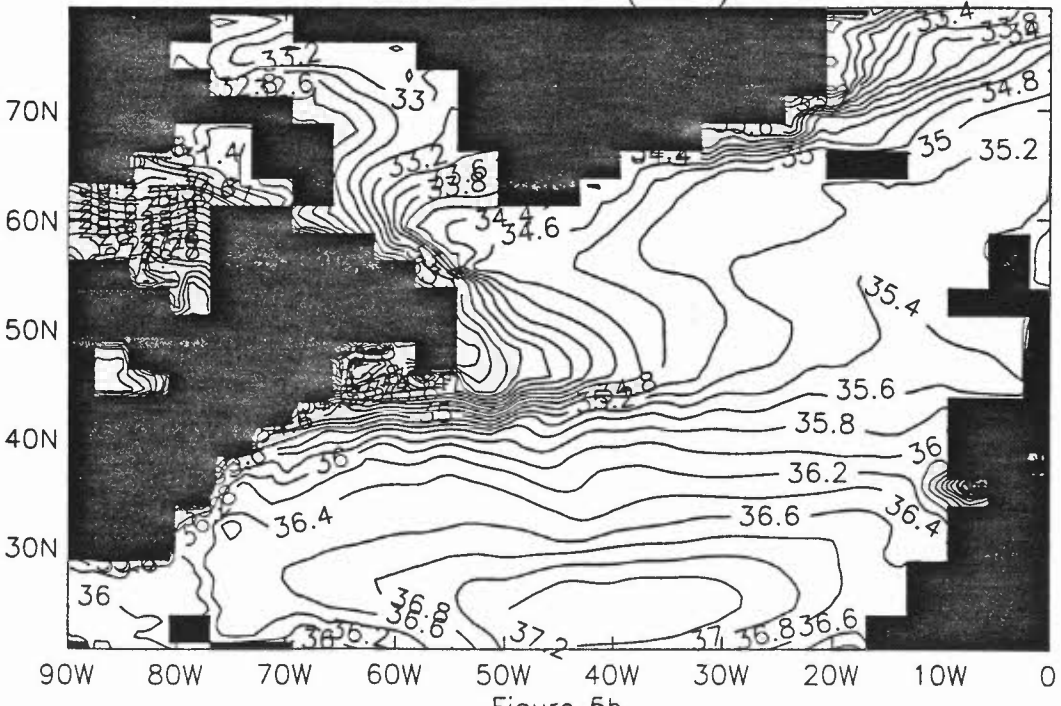

Figure 5b

Levitus (1982) annual mean potential temperature (°C).
Model level 12 (666m).

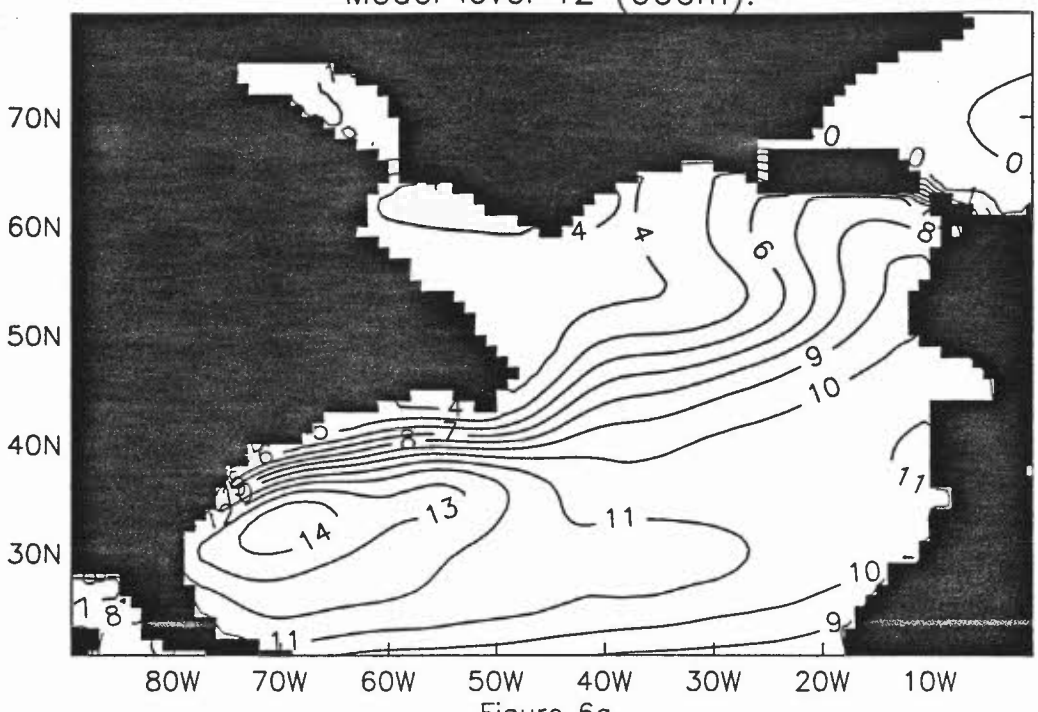
70N
60N
50N
40N
30N
80W
70W
60W
50W
40W
30W
20W
10W
0
4
6
8
9
10
11
13
14
12
7
5
1
Figure 6a.

Levitus (1982) annual mean Salinity (psu).
Model level 12 (666m).

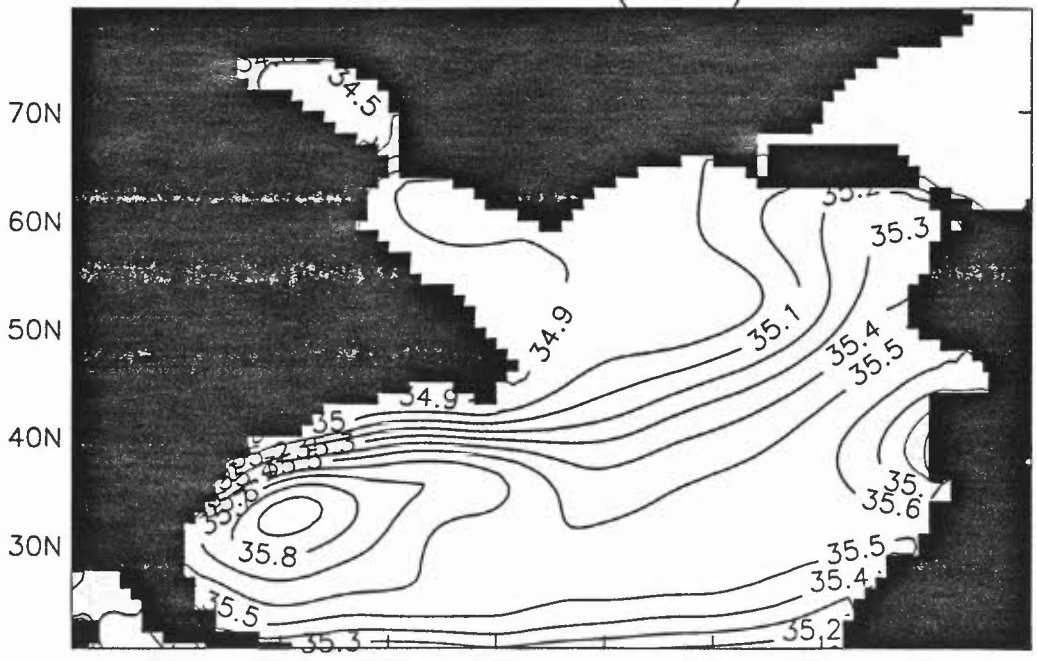
70N
60N
50N
40N
30N
80W
70W
60W
50W
40W
30W
20W
10W
34.5
34.9
35
35.1
35.3
35.4
35.5
35.6
35.8
35.2
Figure 6b.

Control run annual mean potential temperature (°C).
Model level 12 (666m).

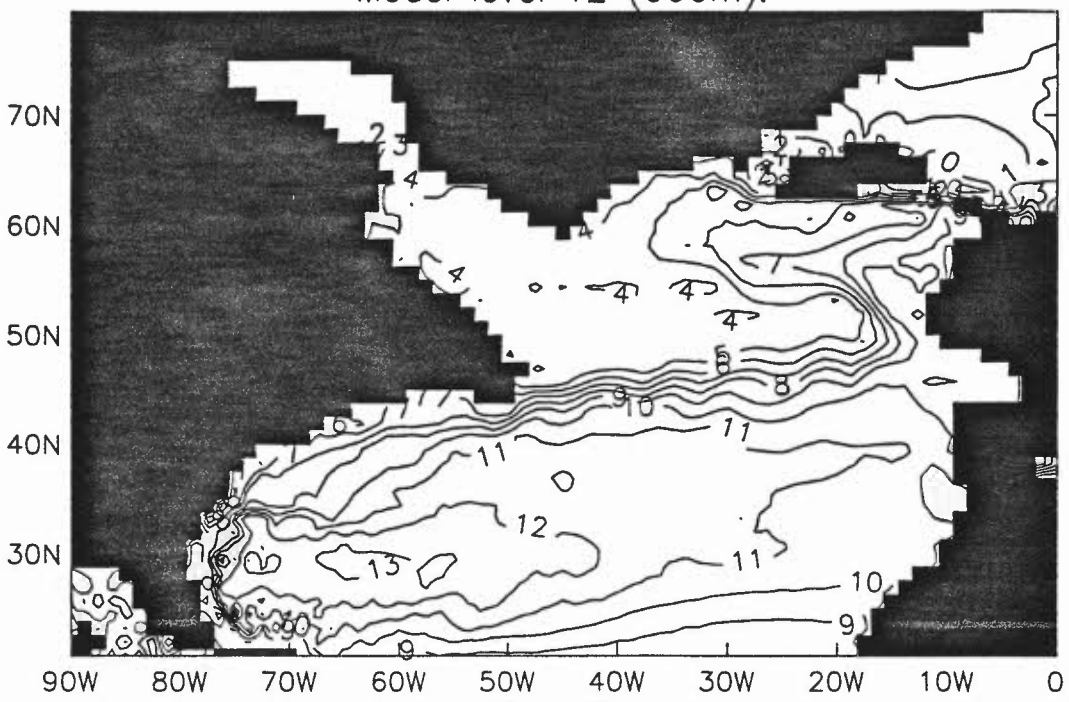

Figure 7a.

Control run annual mean salinity (psu).
Model level 12 (666m).

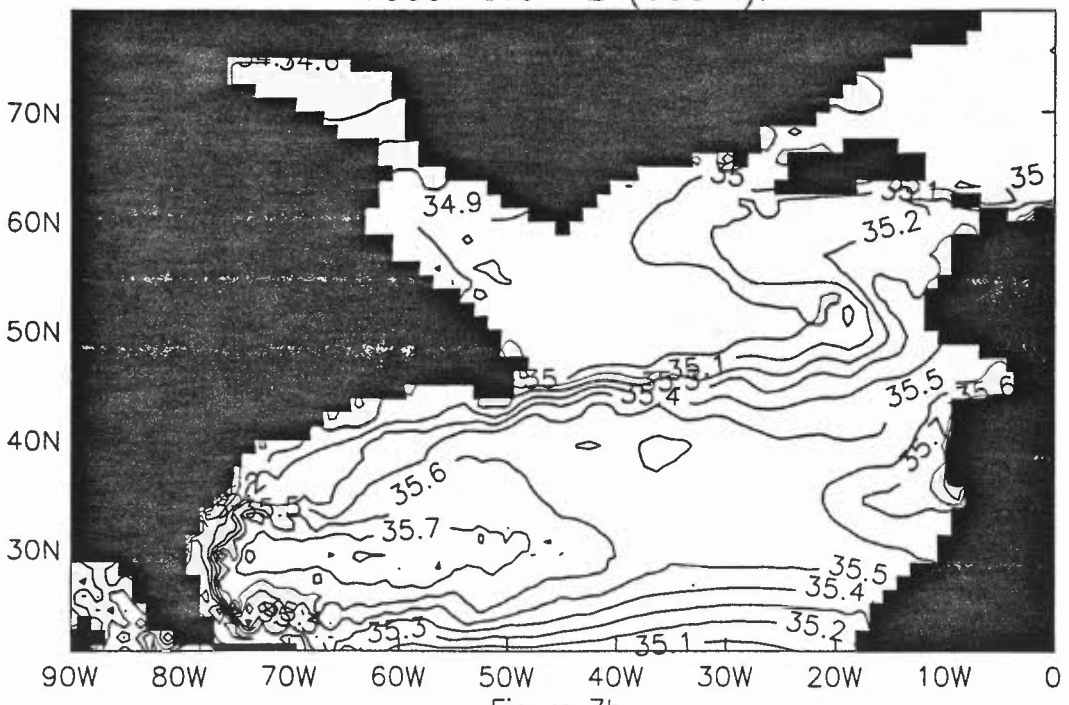

Figure 7b.

Labrador Sea anomaly run annual mean potential temperature (°C).
Model level 5 (47m).

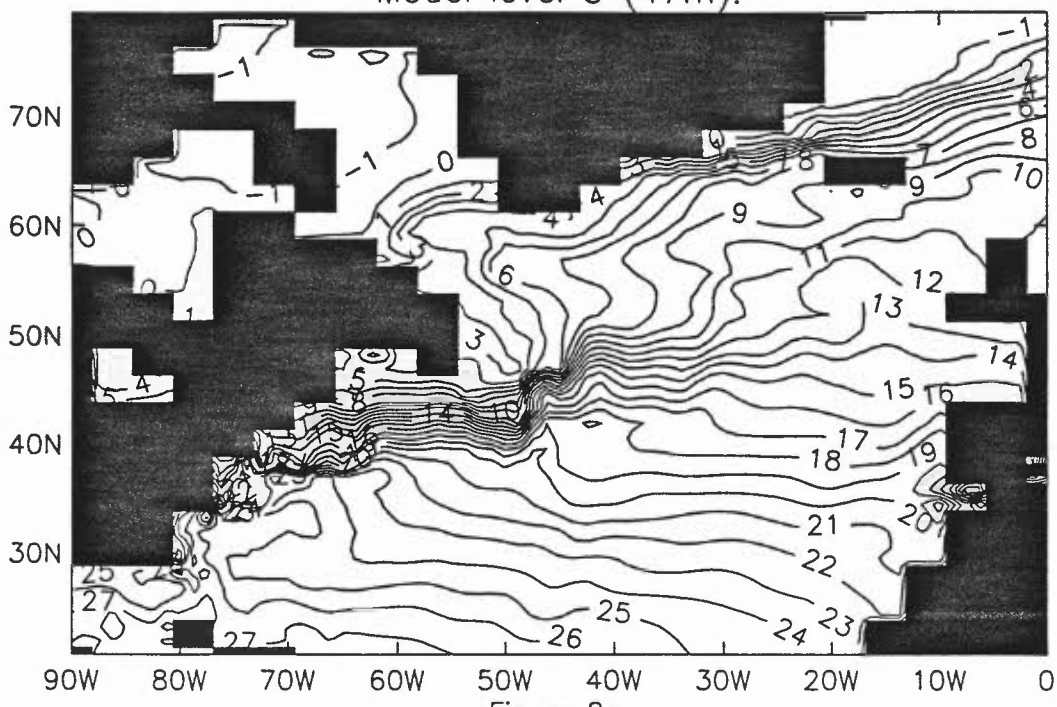

Figure 8a.

Labrador Sea anomaly run annual mean salinity (psu).
Model level 5 (47m).

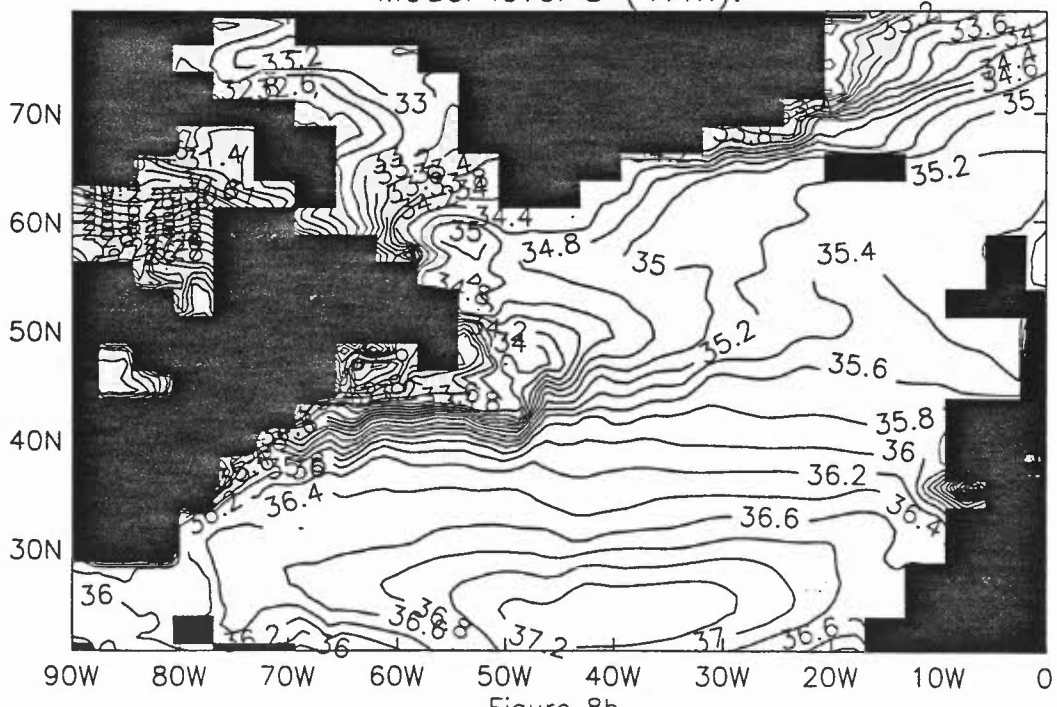

Figure 8b.

Labrador Sea anomaly – control run difference.
Annual mean potential temperature (°C).
Model level 5 (47m).

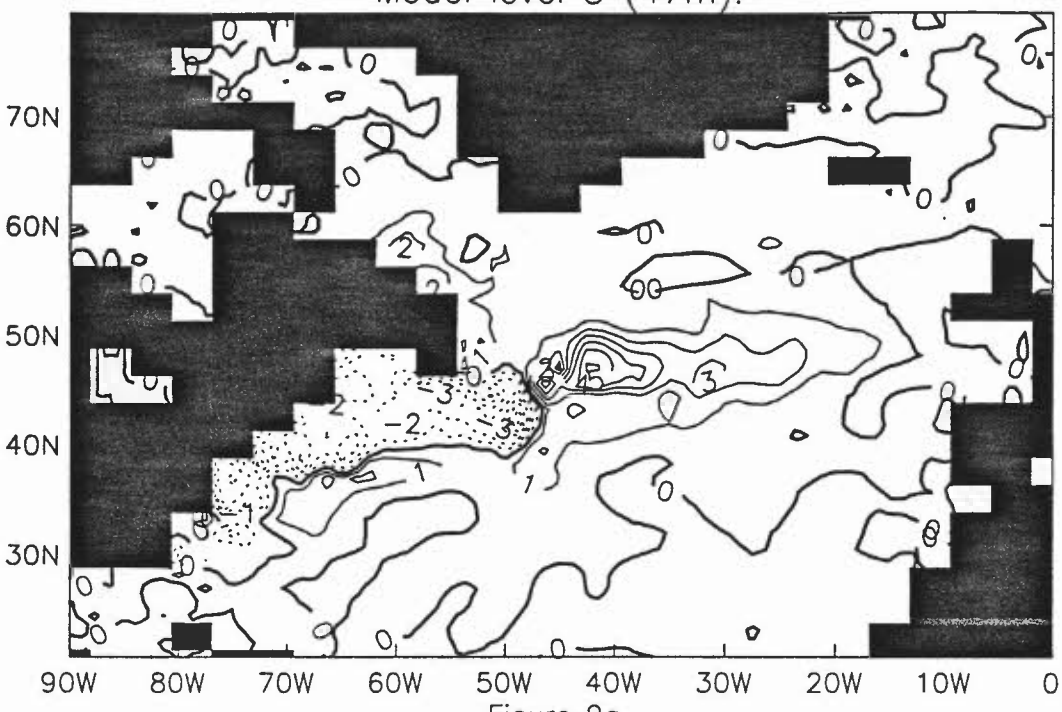

Figure 9a.

Labrador Sea anomaly – control run difference.
Annual mean salinity (psu).
Model level 5 (47m).

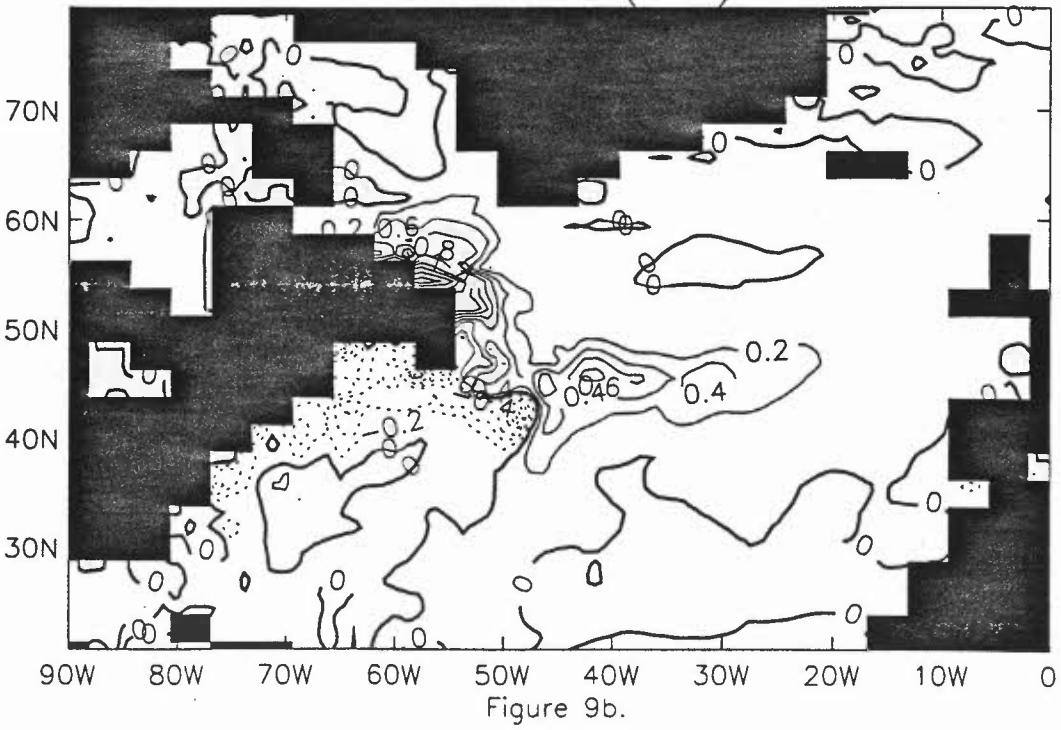

Figure 9b.

Labrador Sea anomaly run annual mean potential temperature (°C).
Model level 12 (666m).

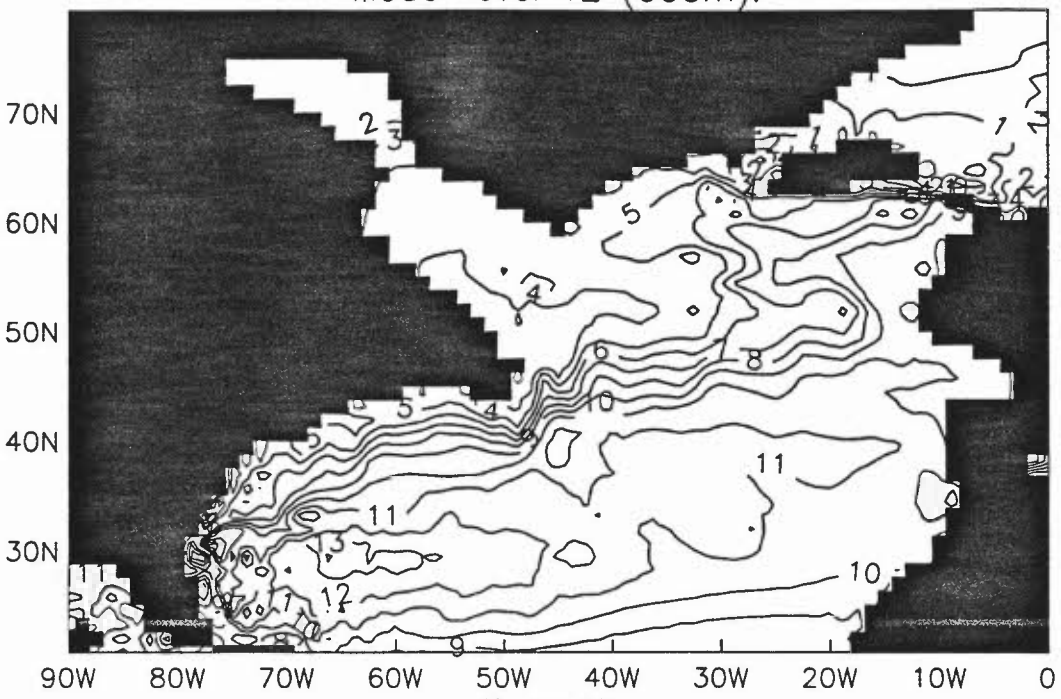

Figure 10a.

Labrador Sea anomaly run annual mean salinity (psu).
Model level 12 (666m).

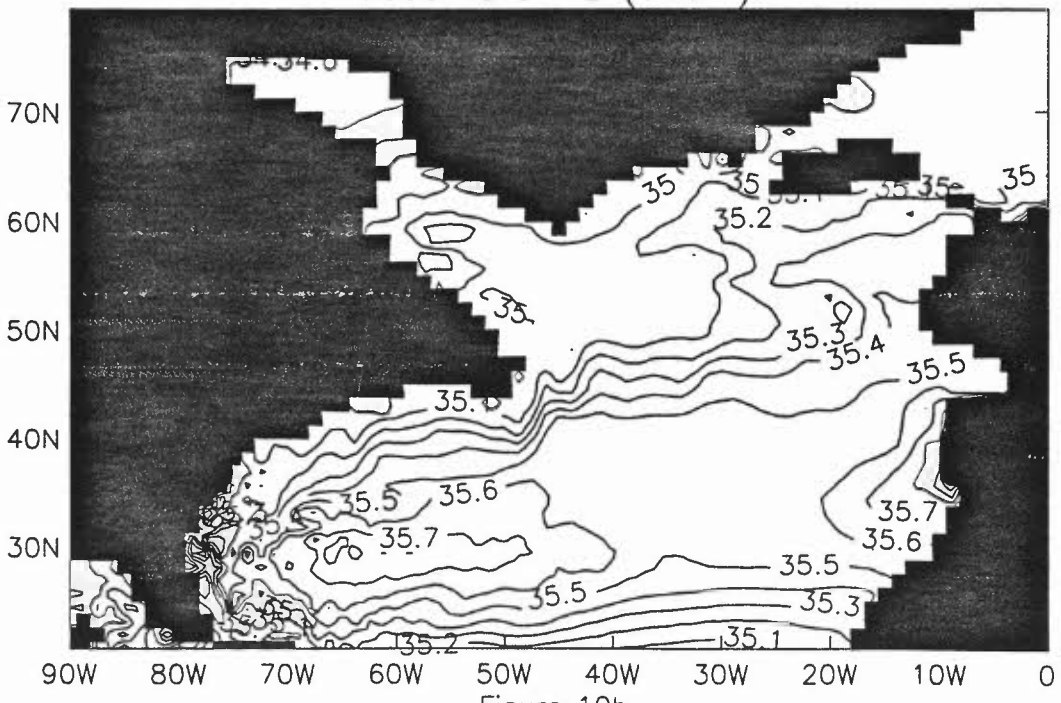

Figure 10b.

Figure 11b. Labrador Sea anomaly run volume transport binned into its respective tracer characteristics across a section shown in figure 3.

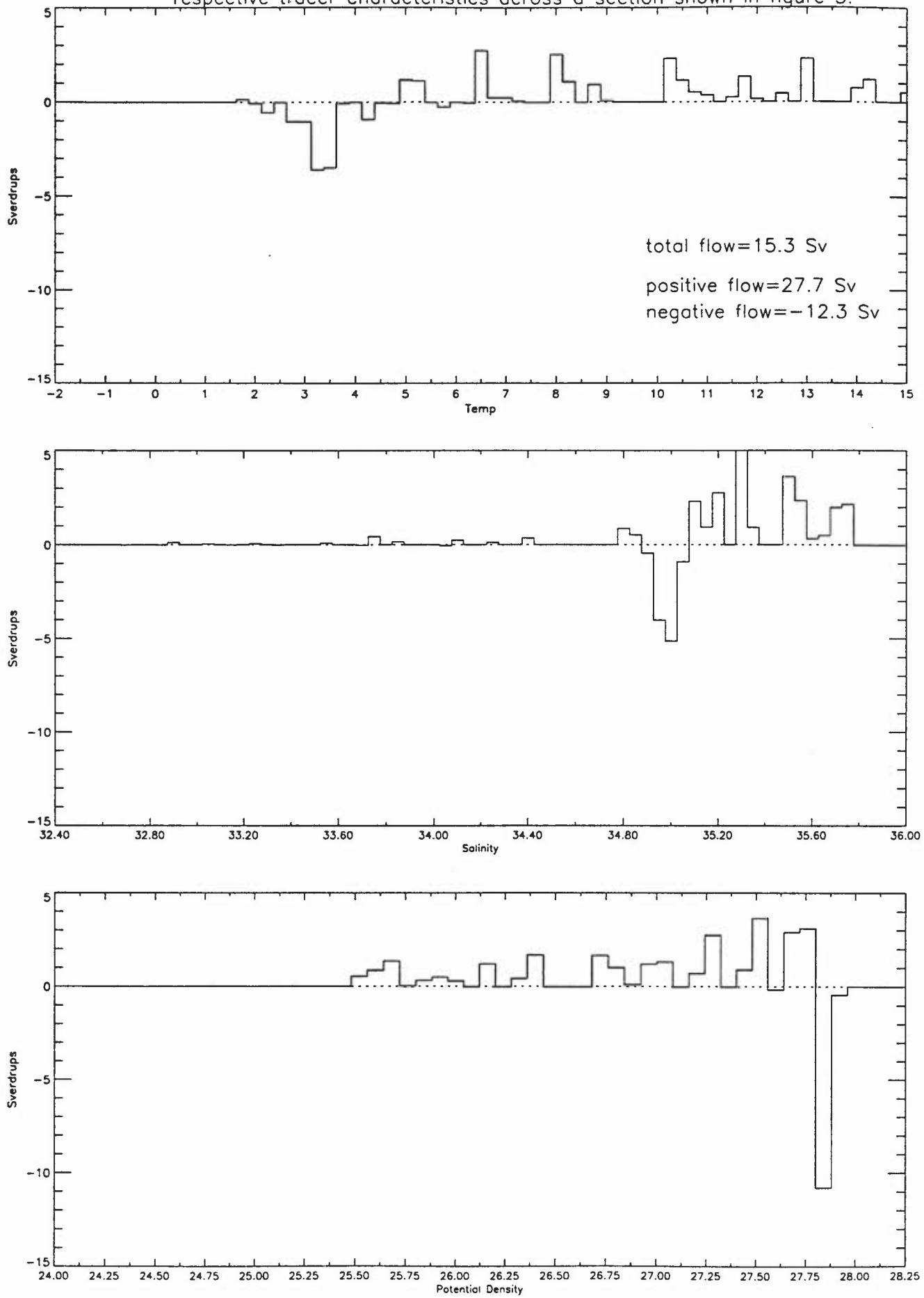

Figure 11a. Control run volume transport binned into its respective tracer characteristics across a section shown in figure 3.

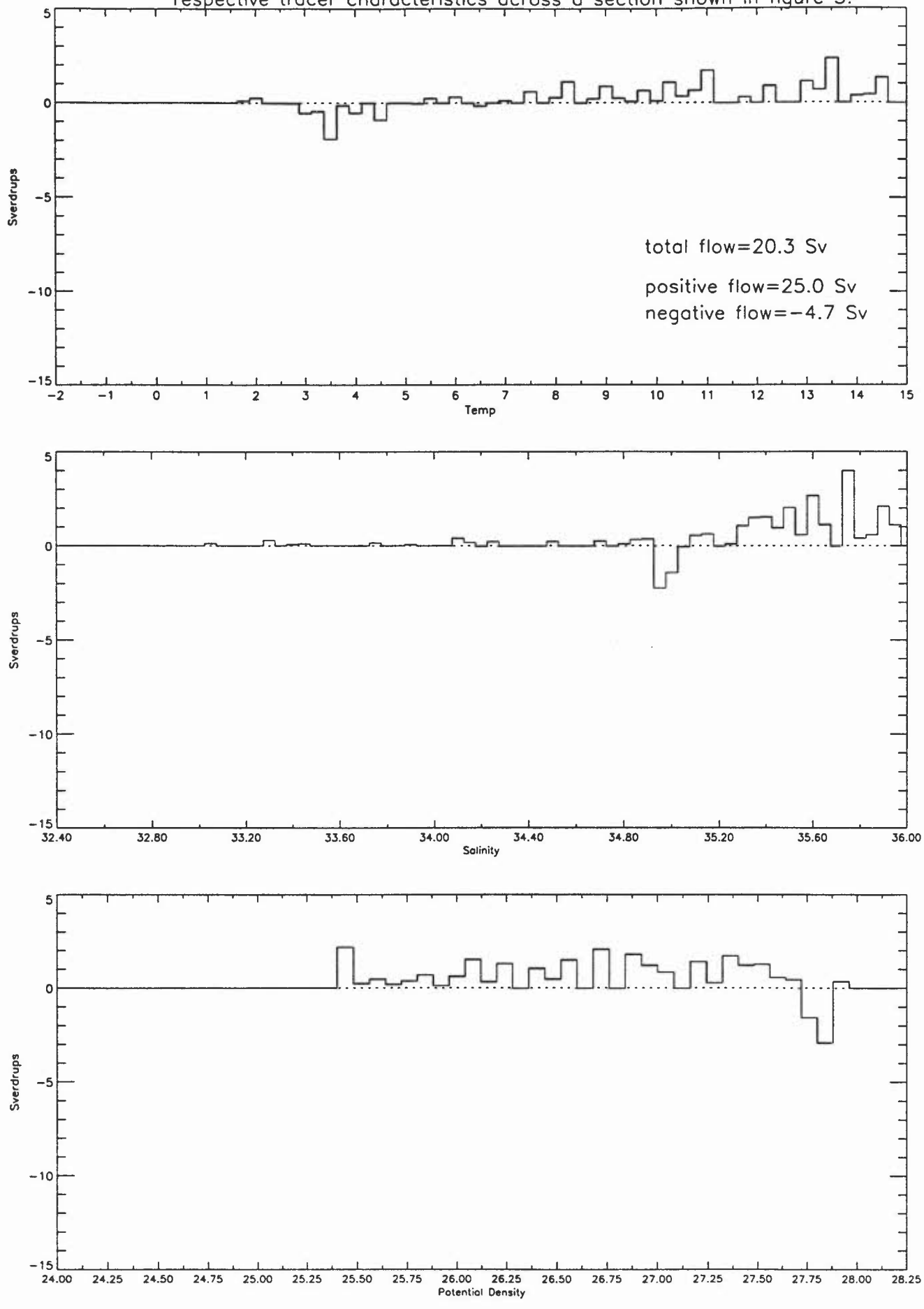

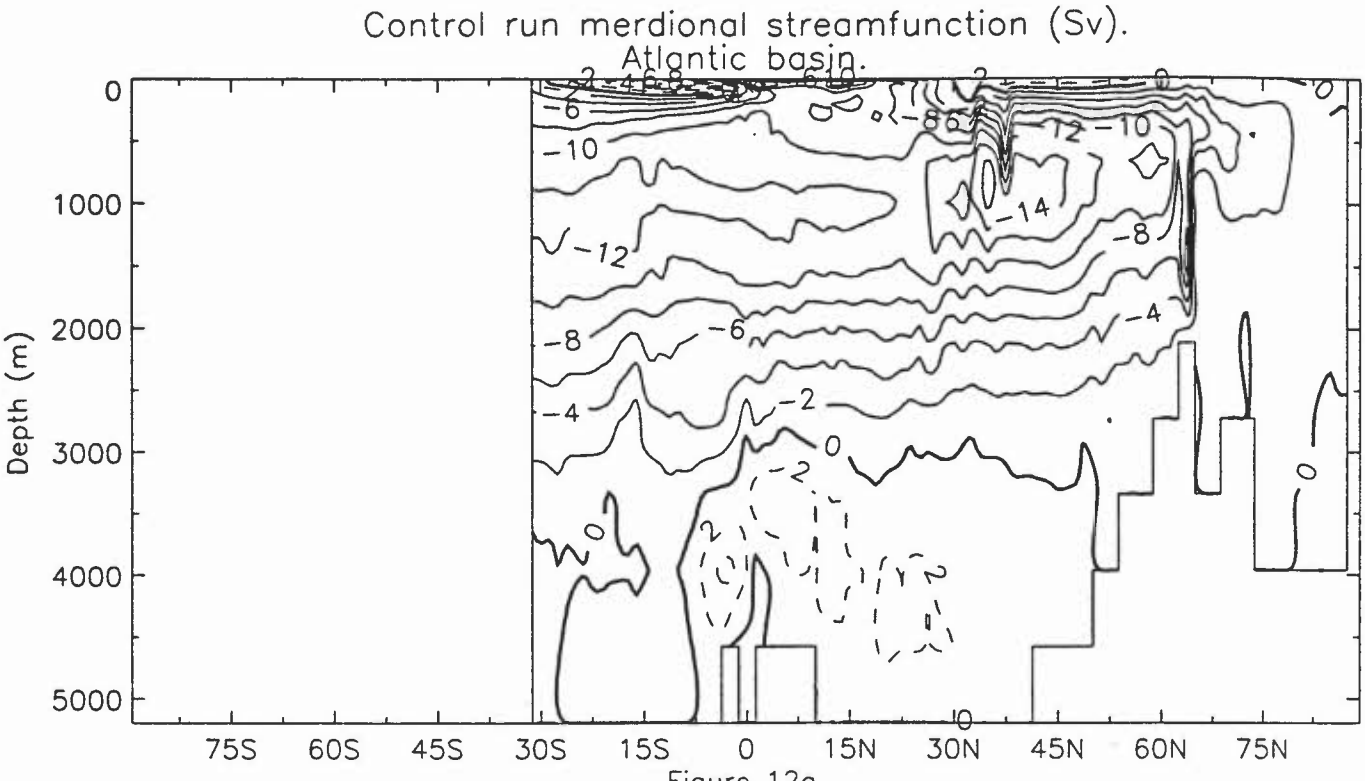

Figure 12a.

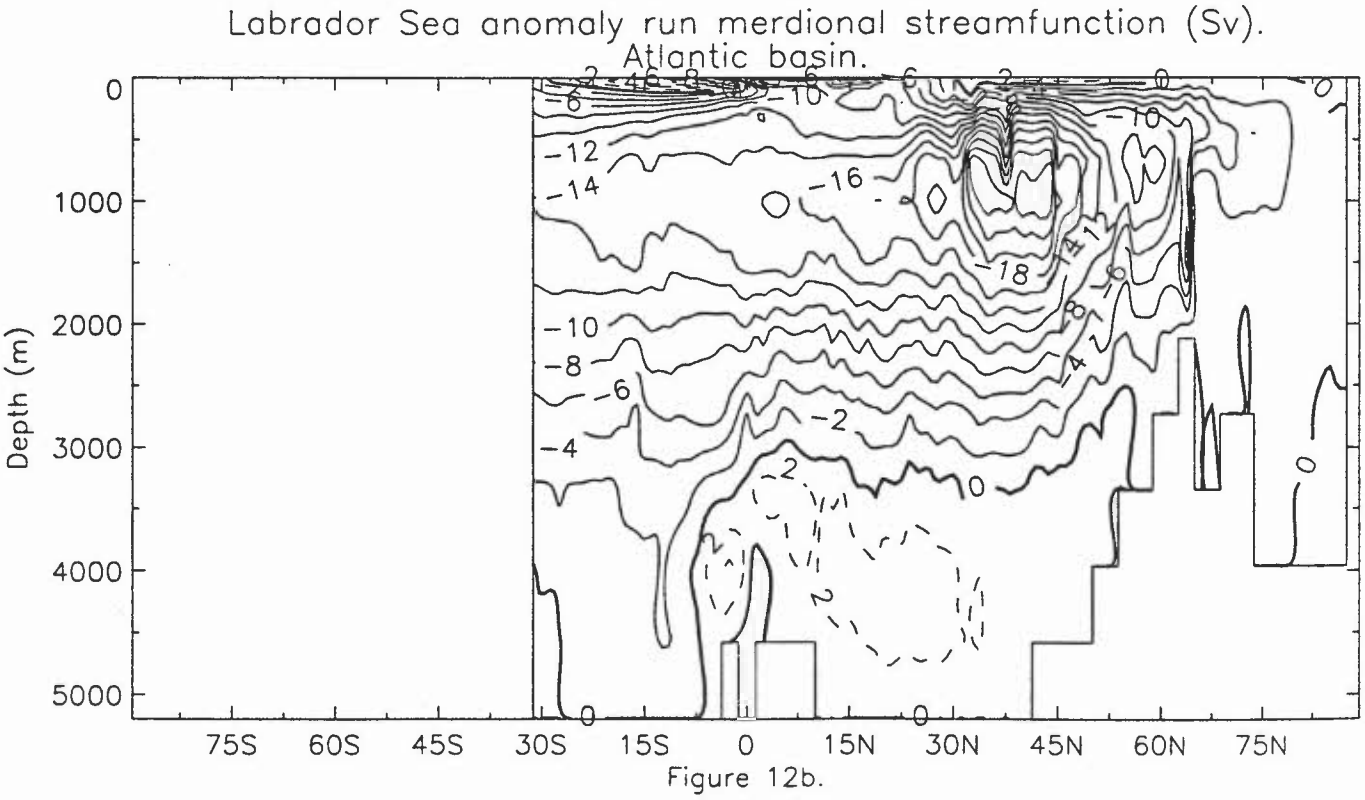

Figure 12b.

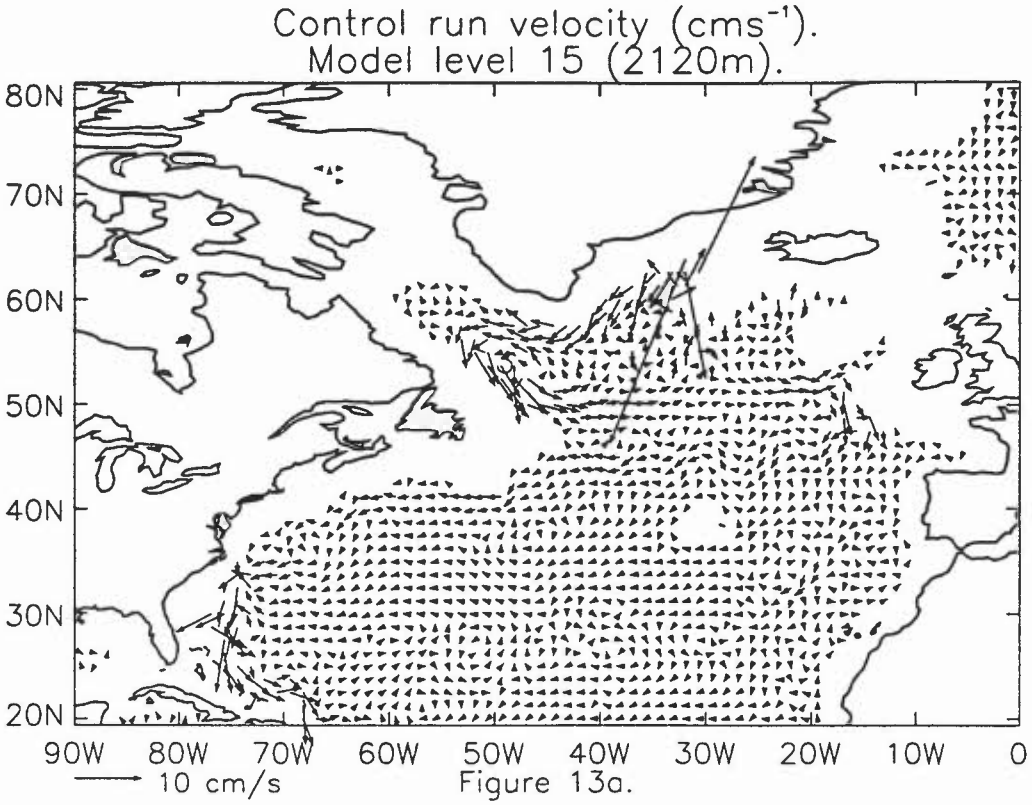

Figure 13a.

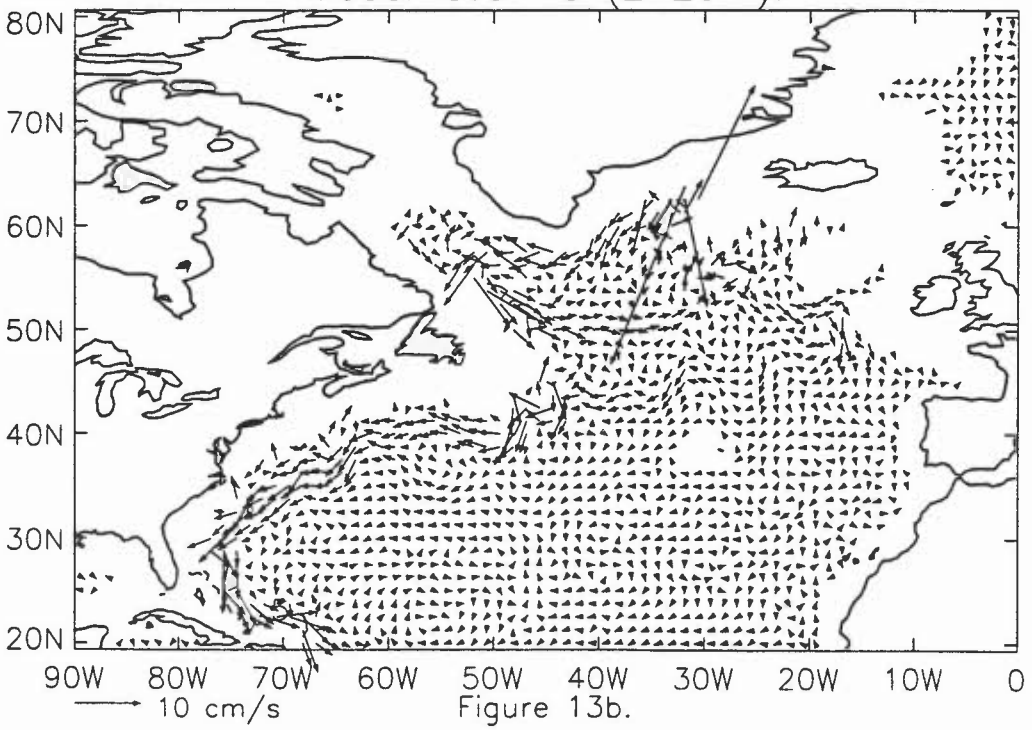

Figure 13b.

Labrador Sea anomaly – control run difference.
Annual mean potential temperature (°C).
Model level 15 (2120m).

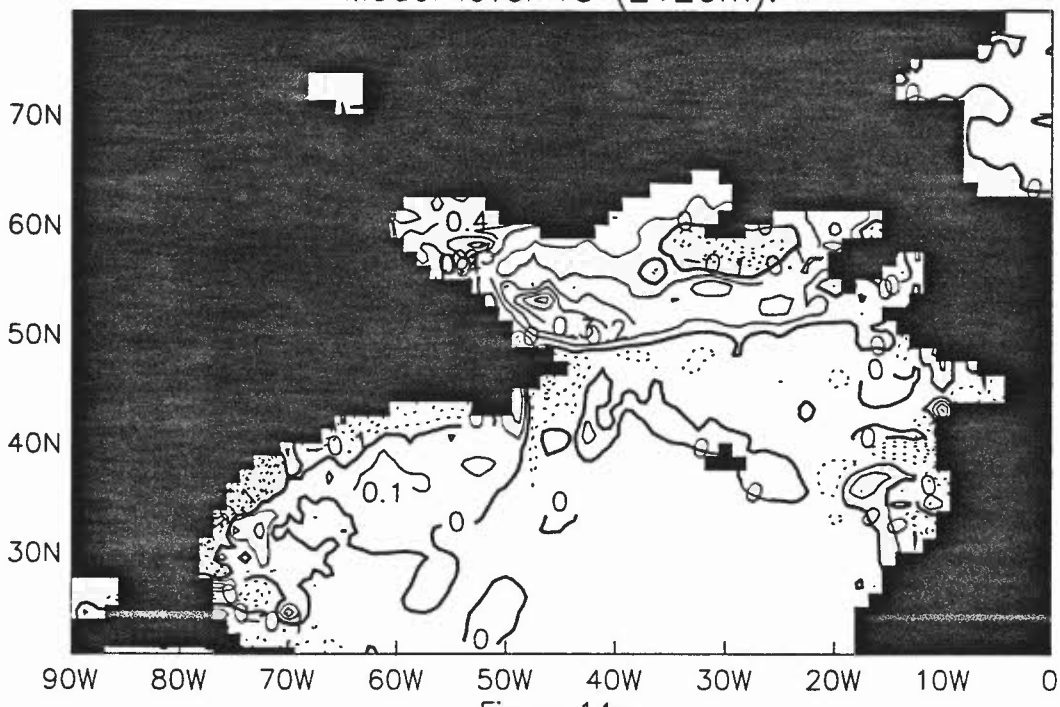

Figure 14a.

Labrador Sea anomaly – control run difference.
Annual mean salinity (psu).
Model level 15 (2120m).

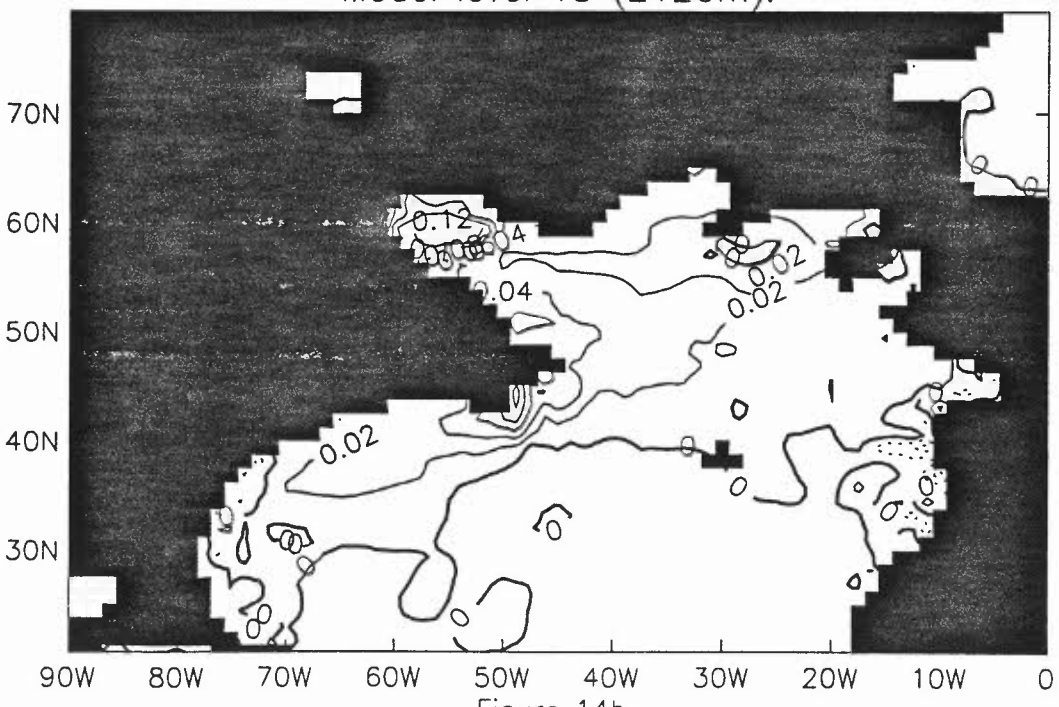

Figure 14b.